

# A Novel All Helix Fold of the AP180 Amino-Terminal Domain for Phosphoinositide Binding and Clathrin Assembly in Synaptic Vesicle Endocytosis

Yuxin Mao,<sup>1</sup> Jue Chen,<sup>2</sup> Jennifer A. Maynard,<sup>4,6</sup>  
Bing Zhang,<sup>5,6</sup> and Florante A. Quiocho<sup>1,2,3,7</sup>

<sup>1</sup>Structural and Computational Biology and  
Molecular Biophysics Graduate Program

<sup>2</sup>Howard Hughes Medical Institute

<sup>3</sup>Department of Biochemistry and Molecular Biology  
Baylor College of Medicine  
Houston, Texas 77030

<sup>4</sup>Department of Chemical Engineering

<sup>5</sup>Section of Neurobiology, Institute for Neuroscience

<sup>6</sup>Institute for Cellular and Molecular Biology  
University of Texas  
Austin, Texas 78712

## Summary

Clathrin-mediated endocytosis plays a major role in retrieving synaptic vesicles from the plasma membrane following exocytosis. This endocytic process requires AP180 (or a homolog), which promotes the assembly and restricts the size of clathrin-coated vesicles. The highly conserved 33 kDa amino-terminal domain of AP180 plays a critical role in binding to phosphoinositides and in regulating the clathrin assembly activity of AP180. The crystal structure of the amino-terminal domain reported herein reveals a novel fold consisting of a large double layer of sheets of ten  $\alpha$  helices and a unique site for binding phosphoinositides. The finding that the clathrin-box motif is mostly buried and lies in a helix indicates a different site and mechanism for binding of the domain to clathrins than previously assumed.

## Introduction

Synaptic transmission requires not only the release of neurotransmitters through exocytosis of synaptic vesicles (SVs), but also the recycling of these vesicles (Heuser and Reese, 1973). At most synaptic terminals, SV recycling is accomplished through clathrin-mediated endocytosis that involves a series of sequential protein and lipid interactions (Schmid, 1997; Zhang and Ramaswami, 1999). The key steps of this endocytic process include assembly of clathrin-coated vesicles, pinching off of these vesicles from the plasma membrane, and removal of clathrin coats to release the nascent vesicles. Following exocytosis, clathrin triskelion and its assembly proteins (APs) AP-2 and AP180 initiate endocytosis of SV components by assembling coated vesicles (Keen et al., 1979; Gonzales-Gaitan and Jackle, 1997; Zhang et al., 1998; Morgan et al., 1999; Nonet et al., 1999). The assembly of coats is further facilitated by endophilin, a lysophosphatidic acid acyl transferase that assists curvature formation by converting inverted cone-shaped lipids into cone-shaped lipids (Ringstad et al., 1999;

Schmidt et al., 1999). Once coated vesicles are formed, they are detached from the plasma membrane to enter the cytoplasm by the dynamin GTPase-amphiphysin complex (Koenig and Ikeda, 1989; Shupliakov et al., 1997; Schmid et al., 1998). These endocytosed vesicles, which only transiently retain their clathrin coats, then undergo a coat removal process so that they can be reloaded with transmitters and poised for the next round of exocytosis. Auxilin, hsc70, and the polyphosphoinositide phosphatase synaptojanin have been proposed to assist in stripping the clathrin coats (Ungewickell et al., 1995; Cremona et al., 1999).

Recently, the regulation of the assembly of clathrin-coated vesicles has received considerable attention. The clathrin assembly protein AP180 appears to be the key player that determines the size of SVs by restricting the size of coated vesicles (Zhang et al., 1999). AP180 represents a growing family of monomeric clathrin assembly proteins that are widely distributed in a variety of organisms (McMahon, 1999). Two isoforms of AP180 are found in yeast, but they do not seem to play a significantly functional role in endocytosis (Wendland and Emr, 1998; Huang et al., 1999). In mammals and humans, two AP180 homologs are found to be either specifically present in presynaptic terminals (Ahle and Ungewickell, 1986; Sousa et al., 1992) or distributed ubiquitously (Dreyling et al., 1996). Unlike in yeast, genetic deletion of AP180 homologs in *Drosophila* (LAP) (Zhang et al., 1998) and in *C. elegans* (UNC-11) (Nonet et al., 1999) significantly impairs SV endocytosis and alters the size of SVs in nerve terminals. Similarly, injection of interfering AP180 peptides into squid giant axons impairs synaptic transmission and alters SV size (Morgan et al., 1999). In vitro neuronal AP180 induces the formation of uniform sized clathrin cages (Ye and Lafer, 1995a), providing further evidence for the role of AP180 in regulating SV size.

At the primary structural level, the AP180s can be divided into two distinct domains, an amino- or N-terminal domain and a carboxy- or C-terminal domain (Murphy et al., 1991; Morris et al., 1993; Ye and Lafer, 1995b). The N-terminal domain (we named “NAP” for N-terminal AP180 domain) of the AP180s contains about 300 highly conserved residues, whereas the C-terminal domain varies significantly both in length (~150 to 600 residues) and similarity among all AP180 homologs (McMahon, 1999). Despite the high degree of conservation and its interaction with clathrin triskelion, the NAP domain does not assemble clathrin (Ye and Lafer, 1995b). Rather, the NAP domain of AP180 appears to play a critical role in regulating the assembly activity of the AP180s, which is mediated by the C-terminal domain. The NAP domain shares three putative modules: a phosphoinositide binding site (Norris et al., 1995; Hao et al., 1997), a clathrin binding site or “clathrin-box” motif (ter Haar et al., 2000), and a leucine zipper (Wendland and Emr, 1998). AP180 binds both inositol (Norris et al., 1995) and phosphatidylinositol polyphosphates (Hao et al., 1997), which negatively regulate the activity of AP180 and inhibit clathrin cage assembly. Binding to phosphoinositide moieties,

<sup>7</sup>To whom correspondence should be addressed (e-mail: faq@bcm.tmc.edu).

Table 1. Crystallographic Analysis Statistics

A. Data Collection							
Crystal	Wavelength (Å)	d <sub>min</sub> (Å)	No. of Measurements	Unique Reflections	Completeness (%)	<I>/<σ>	R <sub>sym</sub> <sup>a,b</sup> (%)
MAD Phasing data	SeMet λ <sub>1</sub> (0.9793)	2.3	244,157	66,748	99.4 (100)	25.0 (5.5)	6.3 (23.1)
	SeMet λ <sub>2</sub> (0.9788)	2.3	246,217	67,191	99.5 (100)	24.0 (4.4)	6.4 (27.1)
	SeMet λ <sub>3</sub> (0.9712)	2.3	248,253	67,292	99.7 (100)	22.9 (3.5)	6.2 (30.1)
Refinement data	SeMet λ <sub>1</sub> (0.9793)	2.2	274,148	38,772	99.6 (100)	33.0 (5.4)	7.6 (33.7)
B. Phasing							
	Observed Diffraction Ratios <sup>c</sup>						
	λ <sub>1</sub>	λ <sub>2</sub>	λ <sub>3</sub>				
λ <sub>1</sub>	0.0677	0.0440	0.0578				
λ <sub>2</sub>		0.0844	0.0462				
λ <sub>3</sub>			0.0661				
Figure of Merit (FOM) before/after solvent flattening			0.64/0.95				
C. Refinement							
Resolution range (Å)	R value <sup>d</sup> (%)	R free <sup>e</sup> (%)	Bond Length Deviation (Å)	Bond Angle Deviation (°)	Bonded Main Chain Atom B Factor rmsd (Å <sup>2</sup> )	Bonded Side Chain Atom B Factor rmsd (Å <sup>2</sup> )	
50–2.2	21.1	25.3	0.012	1.3	4.15	2.32	
<sup>a</sup> Values in parentheses are for the outer resolution shell.							
<sup>b</sup> R <sub>sym</sub> = Σ <sub>h</sub> Σ <sub>i</sub>  I <sub>i</sub> (h) – <I(h)> /Σ <sub>h</sub> Σ <sub>i</sub> I <sub>i</sub> (h).							
<sup>c</sup> Values are <(Δ F ) <sup>2</sup> > <sup>1/2</sup> /< F  <sup>2</sup> > <sup>1/2</sup> .							
<sup>d</sup> R value = Σ( F <sub>obs</sub>   – k  F <sub>cal</sub>  )/Σ F <sub>obs</sub>  .							
<sup>e</sup> R free is obtained for a test set of reflections, consisting of a randomly selected 5% of the data and not used during refinement.							

<sup>a</sup>Values in parentheses are for the outer resolution shell.

<sup>b</sup> $R_{\text{sym}} = \sum_h \sum_i |I_i(h) - \langle I(h) \rangle| / \sum_h \sum_i I_i(h)$ .

<sup>c</sup>Values are  $\langle (\Delta|F|)^2 \rangle^{1/2} / \langle |F|^2 \rangle^{1/2}$ .

<sup>d</sup>R value =  $\sum (|F_{\text{obs}}| - k |F_{\text{calc}}|) / \sum |F_{\text{obs}}|$ .

<sup>e</sup>R free is obtained for a test set of reflections, consisting of a randomly selected 5% of the data and not used during refinement.

as well as to clathrins, may also promote membrane association and proper localization of clathrin near the plasma membrane (Zhang et al., 1998).

The clathrin-box motif, with the canonical sequence L(L,I)(D,E,N)(L,F)(D,E), occurs in several proteins, including AP180s, that are involved in the clathrin coat assembly process and endocytosis (Dell'Angelica et al., 1998; ter Haar et al., 2000). The clathrin box of some of these proteins (e.g., nonvisual arrestins, β3 subunit of AP-3 and epsin) has been demonstrated to bind to the N-terminal domain (td40) of clathrin heavy chain (Goodman et al., 1997; Dell'Angelica et al., 1998; Drake et al., 2000). Moreover, recent crystal structure determination of the td40 complexed with short peptides containing the clathrin-box motif from β-arrestin 2 and AP-3 revealed an extended peptide conformation with the motif bound in the groove between blades 1 and 2 of the β propeller structure of the td40 (ter Haar et al., 2000).

To define the atomic structure and gain molecular insights into the roles of the conserved motifs in AP180-clathrin interactions, we have determined the 2.2 Å crystal structure of the recombinant NAP domain of LAP by X-ray crystallography. The structure reveals a novel fold of the highly conserved NAP domain and a unique site on this fold for binding phosphatidylinositol polyphosphates. Unexpectedly, the structure further shows that the clathrin-box motif is mostly buried and lies in a helix that participates in an intramolecular leucine zipper and a three-helix coiled coil.

## Results and Discussion

### A Prototypic All α Helix Fold of the NAP Domain

The crystal structure of the NAP domain (residues 4–301) was determined by the multiple anomalous dispersion

(MAD) phasing technique (Experimental Procedures and Table 1). The structure, missing the first eighteen disordered residues, is composed entirely of ten α helices and connecting loops, all of varying lengths (Figure 1). The helices are folded roughly into a large triangular-shaped layer of two sheets of about 20 Å thick. The large sheet made up of helices α1, α3, α6, α7, α9, and α10 dominates the structure. The smaller sheet is composed of helices α2, α4, and α8. Many hydrophobic residues occupy the space between the two sheets of helices. Although the entire domain is compact, two different packing arrangements of the α helices are evident (Figure 1). The first four short helices, which constitute less than a third of the entire domain, fold into two two-helix hairpins (α1 and α2 and α3 and α4). These two helix hairpins are similar to the HEAT repeat that is the building unit of several large superhelix-of-helices structures of a variety of domains, proteins, and enzymes (Groves and Barford, 1999). The last five long helices, which constitute the bulk of the NAP domain, form a slightly twisted sheet of four helices (α6, α7, α9, and α10) with the longest helix of the domain (α8) packed diagonally against one side of the sheet. This packing arrangement further gives rise to a left-handed antiparallel triple-helix coiled coil between α7, α8, and α9.

Of the several peptide loops connecting the helices in the NAP structure of LAP, the longest is found between α5 and α6 (Figure 1). In LAP and presumably the squid AP180, this long loop is attributed to the presence of a segment of residues (residues 104 to 129 in LAP), which is missing in the rest of the AP180s (Figure 2). The NAP structure indicates that the segment is located in an isolated tight turn and thus could be dispensed without deleterious effect on the structure.

The entire NAP domain adopts a novel fold. A search

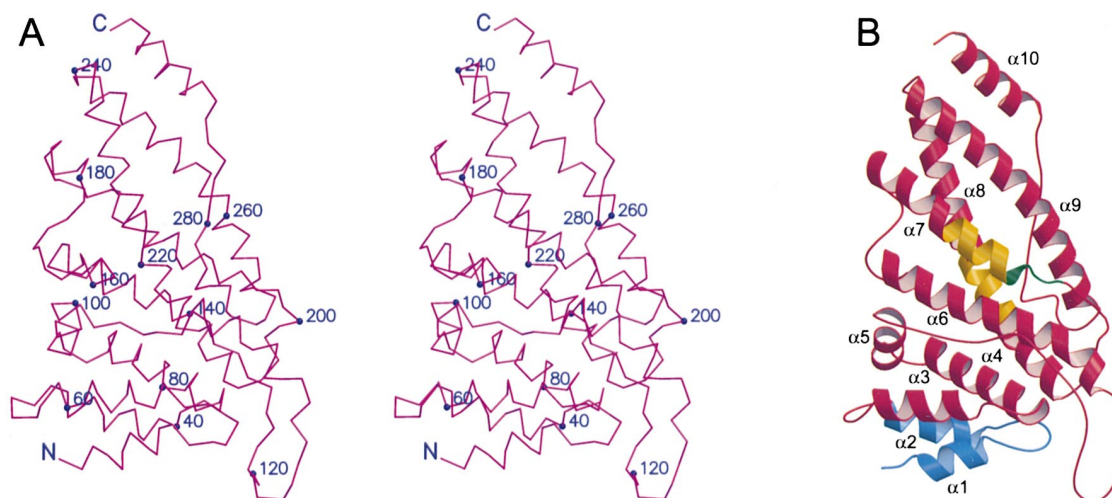


Figure 1. Crystal Structure of the N-Terminal Domain of LAP

(A) Stereo view of the Cα backbone trace with every 20 residues numbered and identified by small filled circles. As residues 4 to 21 are disordered, they are missing from the structure (see Experimental Procedures).

(B) Ribbon representation in the same orientation as in (A) with the ten α helices labeled.

The segment in blue, which includes the two two-helix hairpins (α1 and α2 and α3 and α4), provides a framework for the phosphoinositide binding site. The green segment corresponds to the putative clathrin-box motif present in AP180s (Figure 2) and other clathrin adaptor proteins (ter Haar et al., 2000). The segments (colored yellow) at the C-terminal end of α7 helix and the middle of α8 helix are engaged in an intramolecular antiparallel leucine zipper-like interaction. Figure 2 shows the sequences of the segments associated with the three sites. More detailed views of the sites are shown in Figures 3 and 4. Figures 1, 3A, and 4 were drawn using Molscript (Kraulis, 1991) and Raster3D (Merritt and Bacon, 1997).

for overall structural similarities against the DALI database (Holm and Sander, 1995) failed to reveal any significant matches. The NAP domain structure has shed new light on the three sites that have been implicated in phosphoinositide binding, leucine zipper formation, and clathrin interaction.

#### A Unique Phosphoinositide Binding Site Configuration

It has been proposed that the strongly conserved string of basic residues (KKKH) near the N terminus of the AP180s (<sup>40</sup>KKKH in LAP; Figure 2) is associated with the binding of phosphoinositides (Hao et al., 1997). The domain structure shows that the four basic residues are located in the first turn of helix α2 and its preceding loop and, in combination with two other strongly conserved positively charged residues (K/R26 and K30; Figure 2) residing in helix α1, constitute a large center of positively charged surface well suited for binding inositol polyphosphates (Figures 1, 3A, and 3B). The close proximity and geometry of the two segments of positively charged residues are maintained by an unusual near-circular loop between helices α1 and α2. The unusual configuration of the loop is stabilized by dipolar hydrogen-bonding interactions of its four backbone carbonyl oxygens and completely conserved Thr-32 hydroxyl side chain with the positively charged side chain of the strictly conserved Lys-79 residue from helix α4 (Figures 2 and 3A).

We observed that the structure of the ENTH domain of epsin, which is about half the size of the NAP domain and is folded almost entirely into two HEAT repeats and one three-helix hairpin or an ARM repeat (Hyman et al.,

2000), also exhibits a nearly identical loop geometry and interactions based on the two HEAT repeats. However, the ENTH loop does not contain the cluster of several positively charged residues. We further observed that, although the VHS domain structure of Hrs (Mao et al., 2000) is very similar to that of the ENTH domain (RMSD of 1.8 Å) (Hyman et al., 2000), the dipolar interactions are absent in the equivalent loop of the VHS domain. The local dipolar interactions (with no complementary formal charges) in the circular loops in the NAP (Figure 3A) and ENTH domains stabilize the isolated buried positive charge of the Lys side chain, a mechanism that has been previously observed for the interactions of many uncompensated positive or negative charges buried in proteins (see Pflugrath and Quirocho, 1985; Luecke and Quirocho, 1990; He and Quirocho, 1993, and references therein).

AP180 binds inositol hexakisphosphate and phosphatidylinositol 3,4,5-phosphate as well as 3,4-, and 4,5-phosphates (Norris et al., 1995; Hao et al., 1997). This diverse selectivity is consistent with the location of the binding site mainly on the protein surface and the presence of several flexible positively charged side chains in the site that are capable of making the appropriate electrostatic interactions with the different phosphate substituents of the inositol head group (Figures 3A and 3B). We have been unable thus far to obtain a view of an inositol bound in the crystal. Crystals soaked in or obtained in the presence of inositol hexakisphosphates failed to show ligand binding, owing likely to the presence of a high concentration of competing ammonium sulfate, which was used as precipitant (see Experimental Procedures). However, a direct role of the positively charged center in NAP for phosphoinositide binding is



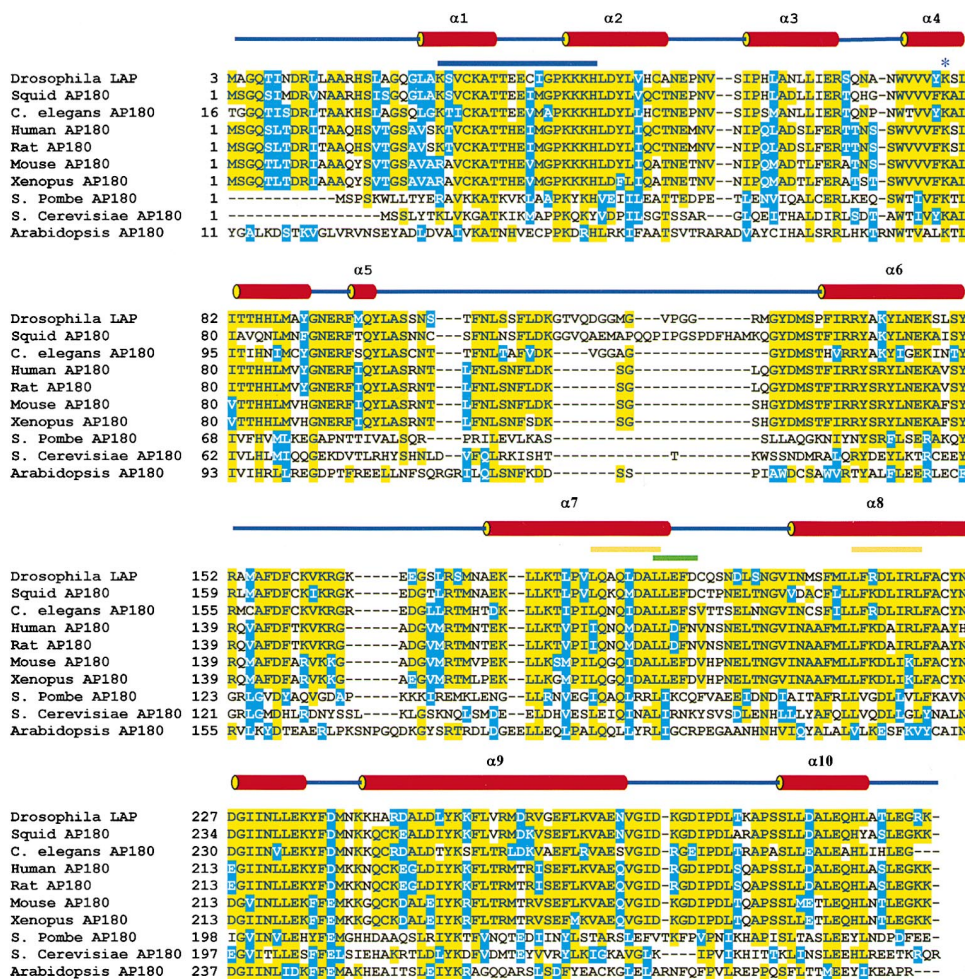


Figure 2. Alignment of the Sequences of the N-Terminal Domain of AP180 Homologs

The  $\alpha$  helices of the LAP structure are shown above the alignment. Identical and very similar residues are highlighted by yellow and blue backgrounds, respectively. The thick colored lines above the alignment identify the segments in LAP that are associated with the various sites in the NAP domain structure as shown in Figures 1, 3, and 4. The blue line covering residues 26–43, which contains several basic residues, indicates the proposed phosphoinositide binding site. This segment is much longer than that deduced by sequence comparison of various AP180 homologs (McMahon, 1999). The putative clathrin binding motif (residues 192–196) is underlined in green. The yellow lines indicate the segments of residues 185–192 and residues 214–221 that are involved in a leucine zipper type interaction based on the NAP structure. The human AP180 is commonly called CALM.

supported by recent studies of the AP180 homolog UNC-11 in *C. elegans*. In *C. elegans*, the q358 allele harbors a deletion that includes the lysine-rich coding region in the NAP domain and extends into an adjacent intron (Nonet et al., 1999). Interestingly, one rare splicing product of q358 has ten amino acids centered on the KKK motif substituted by a different 15-residue segment (A. Alfonso, personal communication). Preliminary results show that a recombinant protein of this mutant deficient in the KKK patch is impaired in phosphoinositide binding but competent in promoting clathrin assembly (E. Lafer and A. Alfonso, personal communication).

The phosphoinositide binding site based on helices in the NAP domain differs completely from those of three other sites that are found in the structures of the pleckstrin homology (PH), C2B, and FYVE domains (Figure 3C). The binding site in the PH domain is located in a cavity formed by loops between  $\beta$  sheet strands (Ferguson et

al., 1995). The high-specificity site in the FYVE zinc finger domain of proteins involved in membrane trafficking and signal transduction resides in a deep and narrow pocket formed mainly between strands from 2-fold symmetric monomers (Mao et al., 2000). The site in the C2B domain  $\beta$  sandwich of synaptotagmins appears to lie on one side of a  $\beta$  sheet (Ibata et al., 1998; Sutton et al., 1999). With the exception of the presence of a large cluster of positively charged residues, all phosphoinositide binding sites (including that in the NAP domain) exhibit different configurations, a reflection of the different folds of the domains (Figure 3C). The PH domain structure is made up of two orthogonal antiparallel  $\beta$  sheets of three and four strands. The FYVE domain consists of two small double-stranded antiparallel  $\beta$  sheets and a C-terminal helix that are held together by two bound  $\text{Zn}^{2+}$ . The C2B domain structure is a  $\beta$  sandwich that closely resembles the immunoglobulin fold.

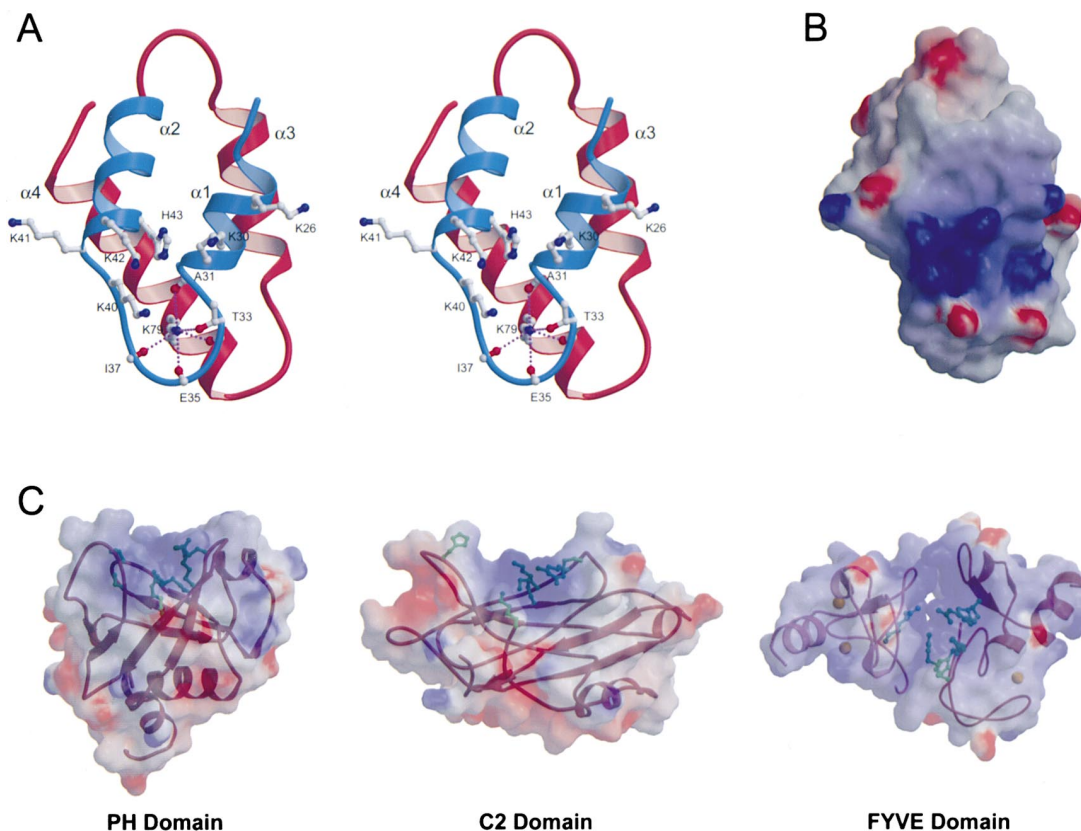


Figure 3. The Phosphoinositide binding Site in the NAP Domain Structure

(A) Stereo view of the phosphoinositide binding site based on the two two-helix hairpins ( $\alpha1$  and  $\alpha2$  and  $\alpha3$  and  $\alpha4$ ). The strongly conserved basic residues (Figure 2) from helices  $\alpha1$  and  $\alpha2$  that form a cluster in the site are shown. None of these residues is involved in electrostatic interactions with other residues. Note the involvement of the positively charged side chain of the strictly conserved Lys-79 from  $\alpha4$  (Figure 2) in hydrogen bonding or dipolar interactions with backbone carbonyl oxygens and a hydroxyl group located in the loop.

(B) Electrostatic surface potential of the region containing the phosphoinositide binding site in the same orientation as in (A). The surface, color-coded according to the potential of red ( $-8kT$ ), white ( $0kT$ ), and blue ( $+8kT$ ), was calculated and displayed using GRASP (Nicholls et al., 1991).

(C) PH, C2B, and FYVE phosphoinositide binding domains. The cluster of basic residues with its intense positive electrostatic surface marks the location of the phosphoinositide binding sites. The PH domain is taken from the structure of phospholipase C with bound inositol trisphosphate (Ferguson et al., 1995) and the FYVE from the structure of the dimeric VHS-FYVE tandem domains (Mao et al., 2000). The C2B domain is based on the structure of synaptotagmin III (Sutton et al., 1999). The location of the phosphoinositide binding site in the C2B domain was based on ligand binding and site-directed mutagenesis studies of neuronal and non-neuronal synaptotagmins (Ibata et al., 1998). The figure was drawn with GRASP.

#### A Leucine Zipper

It has been noted that the NAP domain of the AP180s contains a peptide (residues 218–239 in LAP; Figure 2) that may take part in a leucine zipper for mediating regulation of the AP180s and their association with other proteins (Wendland and Emr, 1998). The NAP structure reveals that the segment constitutes the last two-thirds of the long helix  $\alpha8$  (Figure 1), but it does not resemble a potential leucine zipper partner since the leucine and isoleucine residues do not have the required geometrical spacings. This finding and the fact that the aliphatic residues are mostly buried rule out the participation of the segment in a zipper interaction. However, the structure shows the formation within the domain of a short antiparallel leucine zipper-like interaction between helices  $\alpha8$  and  $\alpha7$  (Figures 1 and 4A). The interaction is between segments of residues 185–192 of helix  $\alpha7$  and residues 214–221 of helix  $\alpha8$ . This intramolecular leucine zipper contributes to the stability of the domain struc-

ture, especially in its local environment, which includes the putative clathrin binding motif (discussed below).

#### A Mostly Buried and $\alpha$ -Helical Clathrin-Box Motif of the AP180s

The demonstration that the NAP domain of the AP180s by itself binds to the clathrin triskelia (Ahle and Ungewickell, 1986; Murphy et al., 1991; Morris et al., 1993; Ye and Lafer, 1995b), as well as to phosphoinositides, indicates that the domain promotes membrane association and recruitment of clathrin near the plasma membrane (Zhang et al., 1998). The NAP domain-clathrin interaction is assumed to be between the clathrin-box motif that is conserved in several clathrin adaptor proteins, including the AP180s, and the N-terminal domain of clathrin heavy chains (Dell'Angelica et al., 1998; ter Haar et al., 2000). The conserved motif ( $^{192}$ LLEFD; Figure 2) in LAP, with its well-defined electron density (Figure 4B), resides in the last turn of the  $\alpha7$  helix and the follow-



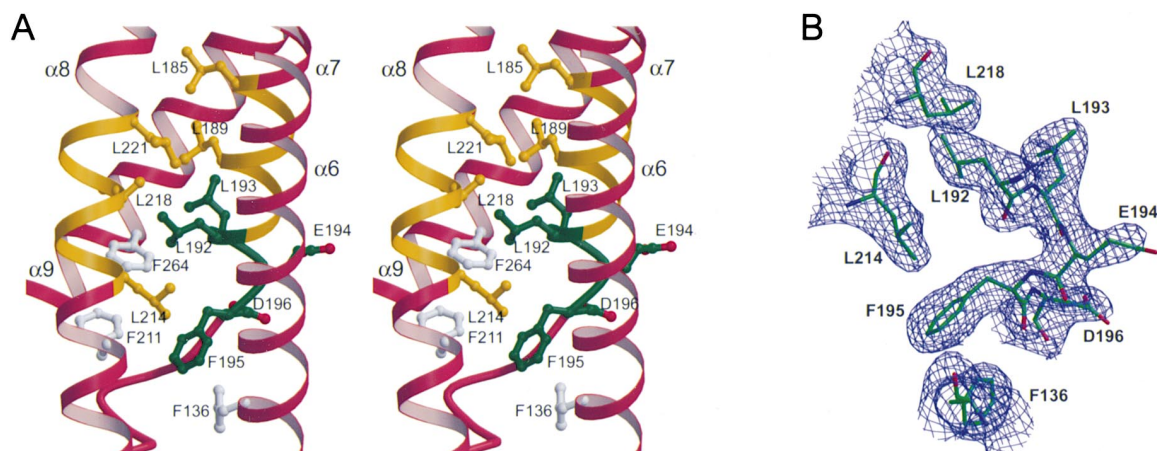


**Figure 4.** An Area Bounded by Helices  $\alpha 6$ ,  $\alpha 7$ ,  $\alpha 8$ , and  $\alpha 9$  that Contains the Putative Clathrin-box motif, Intramolecular Leucine Zipper, and Triple Helix Coiled Coil

(A) Stereo view of the putative clathrin box at the  $\alpha 7$  C terminus and following loop (green), the short antiparallel leucine zipper-like interaction between helices  $\alpha 7$  and  $\alpha 8$  (yellow), and the antiparallel triple-helix coiled coil of helices  $\alpha 7$ ,  $\alpha 8$ , and  $\alpha 9$  (see also Figure 1). Helix  $\alpha 7$  further interacts with helix  $\alpha 6$ . Several hydrophobic residues, notably Phe residues from helices  $\alpha 6$ ,  $\alpha 8$ , and  $\alpha 9$ , are close to the clathrin box.

(B) 2.3 Å electron density map of an area centered on the putative clathrin box calculated with the observed amplitudes and experimental MAD phases (Table 1) and contoured at 1 $\sigma$  level.

ing loop (Figures 1 and 4A). The residues Leu-192, Leu-193, and Phe-195 are completely buried and engaged extensively in interactions with hydrophobic residues, notably Leu and Phe residues (Figure 4A), whereas the two acidic side chains of Glu-194 and Asp-196 are solvent exposed. The stability of the area encompassing the clathrin box is largely provided by the interactions of  $\alpha 7$  with the  $\alpha 6$ ,  $\alpha 8$ , and  $\alpha 9$  helices (Figure 4A). These interactions include the triple-helix coiled coil (Figure 4A) and the leucine zipper between the C-terminal segment of helix  $\alpha 7$ , which contains Leu-192 of the motif, and the middle segment of helix  $\alpha 8$  (Figure 4A).

Our findings came as a complete surprise since the recent crystal structures of the complexes of the N-terminal domain of clathrin (td40) with peptides containing the clathrin box from  $\beta$  arrestin 2 and the  $\beta 3$  hinge of AP-3 both revealed extended conformations for the bound peptides (ter Haar et al., 2000) rather than the partly helical motif we discovered. Moreover, the structures of both complexes show that the motifs are bound in the groove between blades 1 and 2 of the  $\beta$  propeller of the td40 domain mainly through hydrophobic and electrostatic interactions. These bound peptide structures define a general “peptide-in-groove” binding mechanism for the clathrin-box motifs found in many adaptor proteins (ter Haar et al., 2000); however, the segment containing this motif in the NAP domain is unlikely to bind in a similar way, unless it undergoes a very drastic structural rearrangement to expose and reconfigure the motif for docking with the clathrin td40 domain. This rearrangement does not appear possible since our experiments, using chemical crosslinking and plasmon resonance techniques, indicate no significant interactions between the NAP and td40 domains (data not shown). It is interesting to note that the NAP domain in the human AP180 homolog CALM has also been demonstrated to lack the ability to interact with clathrin heavy chain (Tebar et al., 1999). However, these results

do not contradict a role for the interaction of the clathrin box with the td40 domain in clathrin binding as demonstrated for other proteins such as the arrestins, AP-3, and epsin (Goodman et al., 1997; Dell’Angelica et al., 1998; Drake et al., 2000). In addition, motifs similar to the clathrin box have been identified in the C-terminal domain of the mouse and squid AP180s and have been indicated to mediate, by interacting with the td40, clathrin binding and cage assembly (Morgan et al., 2000). Ultimate molecular understanding of the interactions associated with the clathrin box requires the structure determination of the interacting domains.

Our findings argue for a different mechanism for the binding of NAP domain to clathrin, one that may involve a different site in the NAP domain, the clathrin triskelia, or in both. Moreover, given the large double-sided structure of the NAP domain and the location of the phosphoinositide binding site at the edge of the triangle-like structure (Figure 1), there is ample room for additional docking sites. It has been demonstrated that other proteins can bind to the NAP domain of CALM (Tebar et al., 1999). Besides these putative binding partners, the NAP domain is likely to interact with the C-terminal domain to regulate the clathrin assembly activity of the C-terminal domain in SV endocytosis.

## Conclusions

In conclusion, the crystal structure of the NAP domain reported here reveals a novel fold for a domain as large as the average size ( $\sim 35$  kDa) protein and a novel phosphoinositide binding site based on helices and loops. It also indicates that the putative clathrin-box motif is not involved in the binding of the NAP domain to clathrin. The structure provides a sound basis for the study of the interaction of the NAP domain with clathrin triskelia and other potential clathrin assembly proteins and of this domain’s membrane binding and regulatory functions in clathrin assembly.

## Experimental Procedures

### Expression, Purification, and Crystallization

The construct for residues 4–301 of LAP was subcloned into pGEX4T-1 plasmid (Pharmacia) and expressed in *Escherichia coli* BL21 cells. After induction with IPTG for 4 hr at 37°C, cells were harvested and lysed by sonication in PBS buffer with protease inhibitors. The clarified lysate supernatant was passed through a prepackaged glutathione Sepharose 4B column, and washed thoroughly by PBS buffer. The GST tag was removed by thrombin and the protein was further purified using a POROS 20 S cation-exchange column (Perseptive Biosystems). The purified domain of residues 4–301 was crystallized by the hanging drop vapor diffusion method with the drop containing a 1:1 mixture of the protein stock solution (10 mg protein/ml in 1 mM DTT, 50 mM citrate pH (5.5)) and the reservoir solution (30% PEG MME 5000, 200 mM (NH<sub>4</sub>)<sub>2</sub>SO<sub>4</sub>, 100 mM MES (pH 6.8)). Crystals grew in space group C2 with unit cell dimensions of  $a = 105.63 \text{ \AA}$ ,  $b = 106.93 \text{ \AA}$ ,  $c = 79.21 \text{ \AA}$ ,  $\beta = 119.3^\circ$  and two molecules in the asymmetric unit.

### Structure Determination

The structure of the NAP domain (residues of 4–301) was determined by multi-wavelength anomalous dispersion (MAD). Prior to data collection, the crystal was flash-cooled in liquid nitrogen with a cryosolvent consisting of 40% PEG 400, 200 mM (NH<sub>4</sub>)<sub>2</sub>SO<sub>4</sub>, 100 mM MES (pH 6.8). A 3-wavelength data set was collected in 1.5° oscillations from a crystal of selenomethionine-substituted protein on beamline X4A at NSLS of the Brookhaven National Laboratory. The data were processed and merged with DENZO and SCALEPACK, respectively (Otwinowski and Minor, 1997). The positions of 18 of the 22 possible selenium sites (in 2 protein molecules per asymmetric unit) were determined and refined using the suite of programs in CNS (Brünger et al., 1998). An initial model for 260 of the 300 protein residues in both molecules were built using O (Jones et al., 1991) into the 2.4 Å resolution map calculated from MAD phases followed by solvent flattening. The model was refined against the 2.2 Å resolution data (93.4% completeness with 1  $\sigma$  cutoff) in CNS with cycles of model building and fitting of water molecules. As the residues in segments at the N-terminal end (4–21) and in two long loops (117–119 and 163–166) and the last two residues have weak or uninterpretable densities, they were assumed to be flexible. The final model of both molecules contains no unfavorable  $\phi$ ,  $\psi$  combinations. Least square superpositioning of the two molecules in the asymmetric units gave an RMSD of 0.56 Å.

### Acknowledgments

We thank W. E. Meador for technical assistance and C. Ogata for assistance with the MAD data collection at the Brookhaven National Laboratory. We thank Prof. T. Kirchhausen for providing the td40 plasmid and Prof. G. Georgiou for advice and use of facility for the NAP-td40 binding studies. We are also grateful to Profs. E. Lafer and A. Alfonso for communicating experimental results prior to publication. This work was supported in part by a start-up fund to B. Z. from the University of Texas. F. A. Q. is an Investigator in the Howard Hughes Medical Institute.

Received October 27, 2000; revised December 20, 2000.

### References

Ahle, S., and Ungewickell, E. (1986). Purification and properties of a new clathrin assembly protein. *EMBO J.* 5, 3143–3149.  
Brünger, A.T., Adams, P.D., Clore, G.M., DeLano, W.L., Gros, P., Grosse-Kunstleve, R.W., Jian, J.S., Kuszewski, J., Nilges, M., Pannu, N.S., et al. (1998). Crystallography and NMR system: a new software suite for macromolecular structure determination. *Acta Crystallogr. D* 54, 905–921.  
Cremona, O., Di Paolo, G., Wenk, M.R., Luthi, A., Kim, W.T., Takei, K., Daniell, L., Nemoto, Y., Shears, S.B., Flavell, R.A., McCormick, D.A., and De Camilli, P. (1999). Essential role of phosphoinositide metabolism in synaptic vesicle recycling. *Cell* 99, 179–188.  
Dell'Angelica, E.C., Klumperman, J., Stoorvogel, W., and Bonifacino,

J.S. (1998). Association of the AP-3 adaptor complex with clathrin. *Science* 280, 431–434.  
Dreyling, M.H., Martinez-Climent, J.A., Zheng, M., Mao, J., Rowley, J.D., and Bohlander, S.K. (1996). The t(10;11) (p13;14) in the U937 cell line results in the fusion of the *AF10* gene and *CALM*, encoding a new member of the AP-3 clathrin assembly protein family. *Proc. Natl. Acad. Sci. USA* 93, 4804–4809.  
Drake, M.T., Downs, M.A., and Traub, L.M. (2000). Epsin binds to clathrin by associating directly with the clathrin-terminal domain. *J. Biol. Chem.* 275, 6479–6489.  
Ferguson, K.M., Lemmon, M.A., Schlessinger, J., and Sigler, P.B. (1995). Structure of the high affinity complex of inositol trisphosphate with a phospholipase C pleckstrin homology domain. *Cell* 83, 1037–1046.  
Goodman, O.B., Jr., Krupnick, J.G., Vsevolod, V., Gurevich, V.V., Benovic, J.L., and Keen, J.H. (1997). Arrestin/clathrin interaction. Localization of the arrestin binding locus to the clathrin terminal domain. *J. Biol. Chem.* 272, 15017–15022.  
Gonzales-Gaitan, M., and Jackle, H. (1997). Role of *Drosophila*  $\alpha$ -adaptin in presynaptic vesicle recycling. *Cell* 88, 767–776.  
Groves, M.R., and Barford, D. (1999). Topological characteristics of helical repeat proteins. *Curr. Opin. Struct. Biol.* 9, 383–389.  
Hao, W., Tan, Z., Prasad, K., Reddy, K.K., Chen, J., Prestwich, G.D., Falck, J.R., Shears, S.B., and Lafer, E.M. (1997). Regulation of AP-3 function by inositides: identification of phosphatidylinositol 3,4,5-trisphosphate as a potent ligand. *J. Biol. Chem.* 272, 6393–6398.  
He, J.J., and Quirocho, F.A. (1993). Dominant role of local dipoles in stabilizing uncompensated charges on a sulfate sequestered in a periplasmic active transport protein. *Protein Sci.* 2, 1643–1647.  
Heuser, J.E., and Reese, T.S. (1973). Evidence for recycling of synaptic vesicle membrane during transmitter release at the frog neuromuscular junction. *J. Cell Biol.* 57, 315–344.  
Holm, L., and Sander, C. (1995). Dali: a network tool for protein structure comparison. *Trends Biochem. Sci.* 20, 478–480.  
Huang, K.M., D'Hondt, K., Riezman, H., and Lemmon, S.K. (1999). Clathrin functions in the absence of heterotetrameric adaptors and AP180-related proteins in yeast. *EMBO J.* 18, 3897–3908.  
Hyman, J., Chen, H., Di Fiore, P.P., De Camilli, P., and Brünger, A.T. (2000). Epsin undergoes nucleocytoplasmic shuttling and its Eps15 interactor NH<sub>2</sub>-terminal homology domain (ENTH) domain, structurally similar to armadillo and heat repeats, interacts with the transcription factor promyelocytic leukemia Zn<sup>2+</sup> finger protein (PLZF). *J. Cell Biol.* 149, 537–546.  
Ibata, K., Fukuda, M., and Mikoshiba, K. (1998). Inositol 1,3,4,5-tetrakisphosphate binding activities of neuronal and non-neuronal synaptotagmins. *J. Biol. Chem.* 273, 12267–12273.  
Jones, T.A., Zou, J.Y., Cowan, S.W., and Kjeldgaard, M. (1991). Improved methods for building protein models in electron density maps and the location of errors in these models. *Acta Crystallogr. A* 47, 110–119.  
Keen, J.H., Willingham, M.C., and Pastan, I.H. (1979). Clathrin-coated vesicles: isolation, dissociation and factor-dependent reassociation of clathrin baskets. *Cell* 16, 303–312.  
Koenig, J., and Ikeda, K. (1989). Disappearance and reappearance of synaptic vesicle membrane upon transmitter release observed under reversible blockage of membrane retrieval. *J. Neurosci.* 9, 3844–3860.  
Kraulis, P.J. (1991). MOLSCRIPT: a program to produce both detailed and schematic plots of protein structures. *J. Appl. Cryst.* 24, 946–950.  
Luecke, H., and Quirocho, F.A. (1990). High specificity of a phosphate transport protein determined by hydrogen bonds. *Nature* 347, 402–406.  
Mao, Y., Nickitenko, A., Duan, X., Llyod, T.E., Wu, M.N., Bellen, H., and Quirocho, F.A. (2000). Crystal structure of the VHS and FYVE tandem domains of Hrs, a protein involved in membrane trafficking and signal transduction. *Cell* 100, 447–456.  
McMahon, H.T. (1999). Endocytosis: an assembly protein for clathrin cages. *Curr. Biol.* 9, 332–335.

- Merritt, E.A., and Bacon, D.J. (1997). Raster3D, version 2.0: a program for photorealistic molecular graphics. *Meth. Enzymol.* **277**, 505–524.
- Morgan, J.R., Zhao, X., Womack, M., Prasad, K., Augustine, G.J., and Lafer, E.M. (1999). A role for the clathrin assembly domain of AP180 in synaptic vesicle endocytosis. *J. Neurosci.* **19**, 10201–10212.
- Morgan, J.R., Prasad, K., Hao, W., Augustine, G.J., and Lafer, E.M. (2000). A conserved clathrin assembly motif essential for synaptic vesicle endocytosis. *J. Neurosci.* **20**, 8667–8676.
- Morris, S.A., Schroder, S., Plessmann, U., Weber, K., and Ungewickell, E. (1993). Clathrin assembly protein AP180: primary structure, domain organization and identification of a clathrin binding site. *EMBO J.* **12**, 667–675.
- Murphy, J.E., Pleasure, I.T., Puszkun, S., Prasad, K., and Keen, J.H. (1991). Clathrin assembly protein AP-3. The identity of the 155K protein, AP180, and NP185 and demonstration of a clathrin binding domain. *J. Biol. Chem.* **266**, 4401–4408.
- Nicholls, A., Sharp, K.A., and Honig, B. (1991). Protein folding and association: insights from the interfacial and thermodynamic properties of hydrocarbons. *Proteins* **11**, 281–296.
- Nonet, M.L., Holgado, A.M., Brewer, F., Serpe, C.J., Norbeck, B.A., Holleran, J., Wei, L., Hartwig, E., Jorgensen, E.M., and Alfonso, A. (1999). UNC-11, a *Caenorhabditis elegans* AP180 homologue, regulates the size and protein composition of synaptic vesicles. *Mol. Biol. Cell* **10**, 2343–2360.
- Norris, F.A., Ungewickell, E., and Majerus, P.W. (1995). Inositol hexakisphosphate binds to clathrin assembly protein 3 (AP-3/AP180) and inhibits clathrin cage assembly in vitro. *J. Biol. Chem.* **270**, 214–217.
- Pflugrath, J.W., and Quiocho, F.A. (1985). Sulphate sequestered in the sulphate-binding of *Salmonella typhimurium* is bound solely by hydrogen bonds. *Nature* **314**, 257–260.
- Otwinowski, Z., and Minor, W. (1997). Processing of x-ray diffraction data collected in oscillating mode. *Meth. Enzymol.* **276**, 307–326.
- Ringstad, N., Gad, H., Low, P., Di Paolo, G., Brodin, L., Shupliakov, O., and De Camilli, P. (1999). Endophilin/SH3p4 is required for the transition from early to late stages in clathrin-mediated synaptic vesicle endocytosis. *Neuron* **24**, 143–154.
- Schmid, S.L. (1997). Clathrin-coated vesicle formation and protein sorting: an integrated process. *Annu. Rev. Biochem.* **66**, 511–548.
- Schmid, S.L., McNiven, M.A., and De Camilli, P. (1998). Dynamin and its partners: a progress report. *Curr. Opin. Cell Biol.* **10**, 504.
- Schmidt, A., Wolde, M., Thiele, C., Fest, W., Kratzin, H., Podtelejnikov, A.V., Witke, W., Huttner, W.B., and Soling, H.D. (1999). Endophilin I mediates synaptic vesicle formation by transfer of arachidonate to lysophosphatidic acid. *Nature* **401**, 133–141.
- Shupliakov, O., Low, P., Grabs, D., Gad, H., Chen, H., David, C., Takei, K., De Camilli, P., and Brodin, L. (1997). Synaptic vesicle endocytosis impaired by disruption of dynamin-SH3 domain interactions. *Science* **276**, 259–263.
- Sousa, R., Tannery, N.H., Zhou, S., and Lafer, E.M. (1992). Characterization of a novel synapse-specific protein. I. Developmental expression and cellular localization of the F1-20 protein and mRNA. *J. Neurosci.* **12**, 2130–2143.
- Sutton, R.B., Ernst, J. A., and Brünger, A.T. (1999). Crystal structure of the cytosolic C2A–C2B domains of synaptotagmin III. Implications for Ca<sup>2+</sup>-independent snare complex interaction. *J. Cell Biol.* **147**, 589–598.
- Tebar, F., Bohlander, S.K., and Sorkin, A. (1999). Clathrin assembly lymphoid myeloid leukemia (CALM) protein: localization in endocytic-coated pits, interactions with clathrin, and the impact of overexpression on clathrin-mediated traffic. *Mol. Biol. Cell* **10**, 2687–2702.
- ter Haar, E., Harrison, S.C., and Kirchhausen, T. (2000). Peptide-in-groove interactions link target proteins to the -propeller of clathrin. *Proc. Natl. Acad. Sci. USA* **97**, 1096–1100.
- Ungewickell, E., Ungewickell, H., Holstein, S.E., Lindner, R., Prasad, K., Barouch, W., Martin, B., Greene, L.E., and Eisenberg, E. (1995). Role of auxilin in uncoating clathrin-coated vesicles. *Nature* **378**, 632–635.
- Wendland, B., and Emr, S.D. (1998). Pan1p, yeast eps15, functions as a multivalent adaptor that coordinates protein-protein interactions essential for endocytosis. *J. Cell. Biol.* **141**, 71–84.
- Ye, W., and Lafer, E.M. (1995a). Bacterially expressed F1–20/AP-3 assembles clathrin into cages with a narrow size distribution: implications for the regulation of quantal size during neurotransmission. *J. Neurosci. Res.* **41**, 15–26.
- Ye, W., and Lafer, E.M. (1995b). Clathrin binding and assembly activities of expressed domains of the synapse-specific clathrin assembly protein AP-3. *J. Biol. Chem.* **270**, 10933–10939.
- Zhang, B., and Ramaswami, M. (1999). Synaptic vesicle endocytosis and recycling. In *Frontiers in Molecular Biology: Neurotransmitter Release*, H.J. Bellen, ed. (London: Oxford University Press), pp. 389–431.
- Zhang, B., Ganetzky, B., Bellen, H.J., and Murthy, V.N. (1999). Tailoring uniform coats for synaptic vesicles during endocytosis. *Neuron* **23**, 419–422.
- Zhang, B., Koh, Y.H., Beckstead, R.B., Budnik, V., Ganetzky, B., and Bellen, H.J. (1998). Synaptic vesicle size and number are regulated by a clathrin adaptor protein required for endocytosis. *Neuron* **21**, 1465–1475.

#### Protein Data Bank ID Code

Atomic coordinates and structure factor amplitudes have been deposited in the Protein Data Bank (ID code: 1HX8).